J Mol Model (2011) 17:1121–1131
DOI 10.1007/s00894-010-0816-3

ORIGINAL PAPER

A tricotage-like failure of nanographene

Elena F. Sheka · Nadezhda A. Popova · Vera A. Popova · Ekaterina A. Nikitina · Landysh H. Shaymardanova

Received: 12 May 2010 / Accepted: 16 July 2010 / Published online: 3 August 2010

Abstract The response of a nanographene sheet to external stresses was considered in terms of a mechanochemical reaction. The quantum chemical realization of the approach was based on the coordinate-of-reaction concept for the purpose of introducing a mechanochemical internal coordinate (MIC) that specifies a deformational mode. The related force of response is calculated as the energy gradient along the MIC, while the atomic configuration is optimized over all of the other coordinates under the MIC constant-pitch elongation. The approach is applied to the benzene molecule and (5,5) nanographene. A drastic anisotropy in the microscopic behavior of both objects under elongation along a MIC was observed when the MIC was oriented either along or normally to the C–C bond chain. Both the anisotropy and the high stiffness of the nanographene originate from the response of the benzenoid unit to stress.

Keywords Mechanochemical reaction · Mechanochemical internal coordinate · Uniaxial tension · Quantum chemistry · Benzene molecule · Nanographene

Introduction

Much work has been devoted to the calculation of the mechanical properties of nanographenes and carbon nanotubes (CNTs), during the course of which two approaches, namely, continuum and atomistic, have been formulated. The continuum approach is based on the well developed theory of the elasticity of continuous solid media, and is applied to shells, plates, beams, rods, and trusses. The latter are structural elements used for continuum description. When applied to either CNT or nanographene, their cell molecular structure is presented in terms of the above continuum structure elements, and the main task of the calculation is reformulation of the total energy of the studied atomic-molecular nanocarbon system that is being subjected to a change in shape in terms of the continuum structure elements. This procedure involves adaptation of the theory of elasticity of continuous media to nanosize objects that makes allowance for introducing macroscopic basic mechanical parameters such as Young's modulus (E), the Poisson ratio (ν), the potential energy of the elastic deformation, etc., into the description of the mechanical properties of the nanocarbons of interest. Since the energy of these nanocarbons is usually calculated within the framework of modern techniques (Monte-Carlo, molecular dynamics, quantum chemistry), taking into account the object atom structure, the main problem of the continuum approach is the linkage between the molecular configuration and continuum structure elements. Nanoscale continuum methods (see [1–5] and references therein), of which those based on the structural mechanics concept [6] are the most developed, have shown the best ability to simulate nanostructure materials. In view of this concept, CNT and graphene are geometrical frame-like structures where the primary bonds between two nearest-neighboring atoms act like load-bearing beam members, whereas individual atoms act as the joints of the related beams [7–10].

The basic concept of the atomistic approach consists of obtaining the mechanical parameters of the object

E. F. Sheka (✉) · N. A. Popova · V. A. Popova · L. H. Shaymardanova
Peoples' Friendship University of Russia,
117198 Moscow, Russia
e-mail: sheka@icp.ac.ru

E. A. Nikitina
Institute of Applied Mechanics RAS,
119991 Moscow, Russia

from the results of the direct solutions of either Newton motion laws [10, 11] or Schrödinger equations [12, 13] of a certain object that changes its shape following a particular algorithm simulating the desired type of deformation. At this point, it is necessary to note that some of the available calculations were based on quantum chemical calculations, mainly density functional theory (DFT). All the above-cited studies, with the exception of a more recent one [14], were performed within the framework of restricted versions of the programs that do not take into account the spin of graphene odd electrons and thus ignore the correlation interaction between these electrons. The peculiarities of graphene odd electron behavior are connected to the considerable enlargement of its C–C bonds, which, in turn, causes a noticeable weakening of the odd electron interaction and thus requires the correlation interaction between these electrons to be taken into account [15].

In the case of the atomistic approach, it is the forces applied to atoms rather than the energy itself that becomes the main goal of the calculations. These forces are later input into the relations of the macroscopic linear theory of elasticity, and lay the foundation for the evaluation of micro-macroscopic mechanical parameters such as Young's modulus (E^*), the Poisson ratio (ν^*), and so on. It should be mentioned that parameters E and E^*, as well as ν and ν^*, are not the same, and that their coincidence is quite accidental. Obviously, the atomistic approach is less favored compared to the continuum approach due to its time consuming calculations and the fact that it is applicable only to smaller objects. However, it possesses doubtless advantages concerning the description of the mechanical behavior of an object under a certain load (shape changing) as well as exhibiting the deformation and failure process at the atomic level.

Following our wish to emphasize the advantages of the atomistic approach in describing the failure and rupture process of graphene, in the current paper we suggest going beyond a conventional energy-strain-response concept to consider the mechanism of the tensile deformation leading to the failure and rupture of a nanographene sheet as the occurrence of a mechanochemical reaction. The similarity between mechanically induced reaction and first-type chemical reactions, first pointed out by Tobolski and Eyring more than 60 years ago [16], suggested the use of a well developed quantum-chemical (QCh) approach to the reaction coordinates [17] in the study of atomic structure transformation under deformation. First applied to the deformation of poly (dimethylsiloxane) oligomers [18], this approach has proved highly effective in disclosing the mechanism of failure and rupture of various polymers.

Mechanochemical internal coordinates

The main point of the approach concerns the defining of reaction coordinates. When dealing with chemical reactions, the coordinate selected is usually an internal one (valence bond, bond angle or torsion angle) or is presented as a linear combination of the latter. Similarly, mechanochemical internal coordinates (MICs) were introduced as modified internal coordinates defined in such a way as to be able to specify the considered deformational modes [18, 19]. The MICs thus designed should meet the following requirements:

1. Every MIC is a classifying mark of a deformational mode: uniaxial tension and contraction are described by linear MICs similar to valence bonds, bending is characterised by a MIC similar to valence angle, and screwing is attributed to MICs similar to torsional angles. Thus, introduced MICs are microscopic analogues of the macroscopic elements of structural mechanics [6].
2. Every MIC is determined in much the same way as the other internal coordinates except for a set of specifically selected support atoms.
3. The MIC relevant to a particular deformational mode is excluded from the QCh optimisation procedure when seeking the minimum of the total energy.
4. The force of response is determined as the residual gradient of the total energy along the selected MIC. This logic is dictated by the general architecture of conventional QCh software, where the force calculation, namely the total energy gradient calculation, is the key procedure.

Implementation of the MIC concept within the framework of DYQUAMECH software [20], which is based on the Hartree-Fock unrestricted version of the CLUSTER-Z1 codes exploiting advanced semiempirical QCh methods [21], provides (1) the MIC input algorithm, (2) computation of the total energy gradients both in Cartesian and internal coordinates, and (3) optimization of the performance of internal coordinates. Additionally, the program retains all the features of the broken symmetry approach, which is particularly important for treating the odd electronic systems of CNTs [22] and graphene [15].

Force of response calculation

The forces, which are the first derivatives of the electron energy $E(R)$ over the Cartesian atom coordinates R, can be determined as [18]

$$\frac{dE}{dR} = <\phi\left|\frac{\partial H}{\partial R}\right|\phi> + 2<\frac{\partial\phi}{\partial R}|H|\phi> + 2<\frac{\partial\phi}{\partial P}|H|\phi>\frac{dP}{dR} \qquad (1)$$

Here, H represents the adiabatic electron Hamiltonian, φ is the electron wave function of the ground state, and P is

the nucleus momentum. Derivatives are determined for fixed atomic positions. When calculating Eq. 1, a quite efficient computational technique suggested by Pulay [23] was applied. When the force calculation is completed, the gradients are re-determined within the system of internal coordinates in order to proceed further in seeking the total energy minimum by atomic structure optimization. The DYQUAMECH algorithm of force determination concerns forces applied to each of i MICs. These partial forces F_i are then used to determine all the desired micro-macroscopic mechanical characteristics, among which we chose the following characteristics related to uniaxial tension:

$$\text{Force of response } F: \qquad F = \sum\nolimits_i F_i \tag{2}$$

$$\text{Stress } \sigma: \qquad \sigma = F/S = \left(\sum\nolimits_i F_i\right)/S, \tag{3}$$

where S is the loading area,

$$\text{Young's modulus E*:} \qquad \mathrm{E}^* = \sigma/\varepsilon, \tag{4}$$

where $\varepsilon = \Delta L_i/L_0$ is the strain, while ΔL_i is the elongation of the i-th MIC and is identical to all MICs in the current experiment,

$$\text{Stiffness coefficient } k: \qquad k = F/\Delta L_i. \tag{5}$$

The following characteristics are thus obtained when a computational cycle is completed.

1. The atomic structure of the loaded body at any stage of the deformation including bond scission and post-breaking relaxation. Post-breaking fragments can be analysed easily by specifying them as the products of either homolytic or heterolytic reaction. Additional characteristics of the fragments are given in terms of the total N_D and the atomically partitioned N_{DA} numbers of effectively unpaired electrons [24], which is a measure of the fragment radicalization and discloses the chemical reactivity of the fragment atoms.
2. A complete set of dynamic characteristics of the deformation expressed in terms of microscopic and micro-macroscopic characteristics. The former concern energy-elongation, force-elongation, N_D and/or N_{DA}, i.e., elongation responses that exhibit mechanical behaviour of the object at all stages of the deformation considered at the atomic level. The latter involve stress-strain interrelations in terms of Eqs. 3–5 that allow for introduction of convenient mechanic characteristics similar to those of elasticity theory.

The following sections present a selected set of the above-listed topics with respect to tensile deformation of (5,5) nanographene. The calculations were performed using version PM3 of the DYQUAMECH program.

Results and discussion

Graphene as the object of mechanical deformation

From the mechanical viewpoint, the benzenoid hexagon structure of graphene poses two questions from the very beginning concerning: (1) the mechanical properties of the benzenoid unit itself and its mechanical isotropy, in particular; and (2) the influence of the unit packing on the mechanical properties of graphene as a whole. When dealing with the mechanical properties of graphene, the mechanical properties of benzenoid units are conventionally considered as completely isotropic due to the high degree of symmetry of the unit structure [1–14]. However, as shown recently [15], the exact symmetry of the unit in real nanographenes is much lower than D_{6h} thus the suggestion of its mechanical isotropy is rather questionable. Moreover, any conclusion about mechanical isotropy does not necessarily follow from the structural symmetry of an object since rupture of the object is connected with the scission of particular chemical bonds whose choice is determined by the configuration of the relevant MICs that suit the geometry of the loading applied. That is why the surroundings of chemical bonds thus chosen may differ under deformation in different directions even in high symmetry structures.

As for the second question, the anisotropy of the mechanical behavior of benzenoid-based nanocarbons is known, as best revealed by uniaxial tension along zig-zag (zg, parallel to C–C bond) and arm chair (ach, normal to C–C bond) edges of both CNTs [2, 25] and rectangular graphene sheets or ribbons [4, 26]. To check if the anisotropy is connected with the mechanical response of the benzenoid units let us look at the deformation of the benzene molecule subjected to either the *zg* or *ach* mode of uniaxial tension.

Tensile deformation and rupture of the benzene molecule

The configurations of two MICs related to each of the two deformation modes are shown in Fig. 1. The deformation proceeds as a stepwise elongation of the MICs with an increment δL=0.05 Å at each step so that the current MIC length constitutes $L = L_0 + n\delta L$, where L_0 is the initial length of the MIC, and n the number of deformation steps. One end of each MIC is fixed (on atoms 1,2 and 1,5 in the case of *ach* and *zg* modes, respectively). Consequently, these atoms are immobilized while atoms 5,6 and 2,6 move

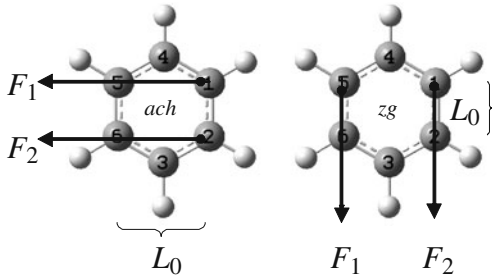

Fig. 1 Two mechanochemical internal coordinates (MICs) of uniaxial tension of the benzene molecule in the *ach* and *zg* deformational modes. L_0 Initial length of MIC; F_1 and F_2 corresponding forces of response

along the arrows leading to successive MIC elongation but do not participate in the optimization procedure at each elongation step.

Figure 2 presents the elongation response dependencies, related to the *ach* and *zg* deformation modes, of the total response force F in terms of Eq. 2 (Fig. 2a), the total N_D (Fig. 2b), and partial N_{DA} (Figs. 2c,d) numbers of unpaired electrons [24] that are the main microscopic characteristics of the mechano-chemical reaction describing benzene molecule failure obtained directly from QCh calculations. Effectively unpaired electrons are just another facet of the spin density, ρ, determined in [14]. Since both spin-polarized DFT in [14] and Hartree-Foch technique in the current study belong to single-determinant unrestricted broken symmetry techniques [22, 24], the appearance of an extra spin density in the singlet state is just a manifestation of the spin-mixed character of the UBS solutions. It has nothing with magnetic properties of the subject [15] heralded in [14] but can be self-consistently used to describe the reactivity of the object atoms in terms of effectively unpaired electrons of total number N_D and partially distributed over atoms N_{DA} both in unstrained state and under deformation.

As seen in Fig. 2, the mechanical behavior of the molecule is highly anisotropic. The force-elongation dependence shown in Fig. 2a differs both in the initial linear region and in the final steps, exhibiting a considerable enlargement of the failure zone in the case of the *zg* mode in comparison with the *ach* mode. Linear elastic behavior is highly restricted and is limited to one or two first deformation steps. An even more radical difference is illustrated in Figs. 2b–d, pointing to the difference in the electronic processes that accompany failure of the molecule. Obviously, these features are connected to the difference in MIC atomic composition related to the two modes, which results in a difference in the molecular fragments formed under rupture. In the case of the *zg* mode, two MICs are aligned along the

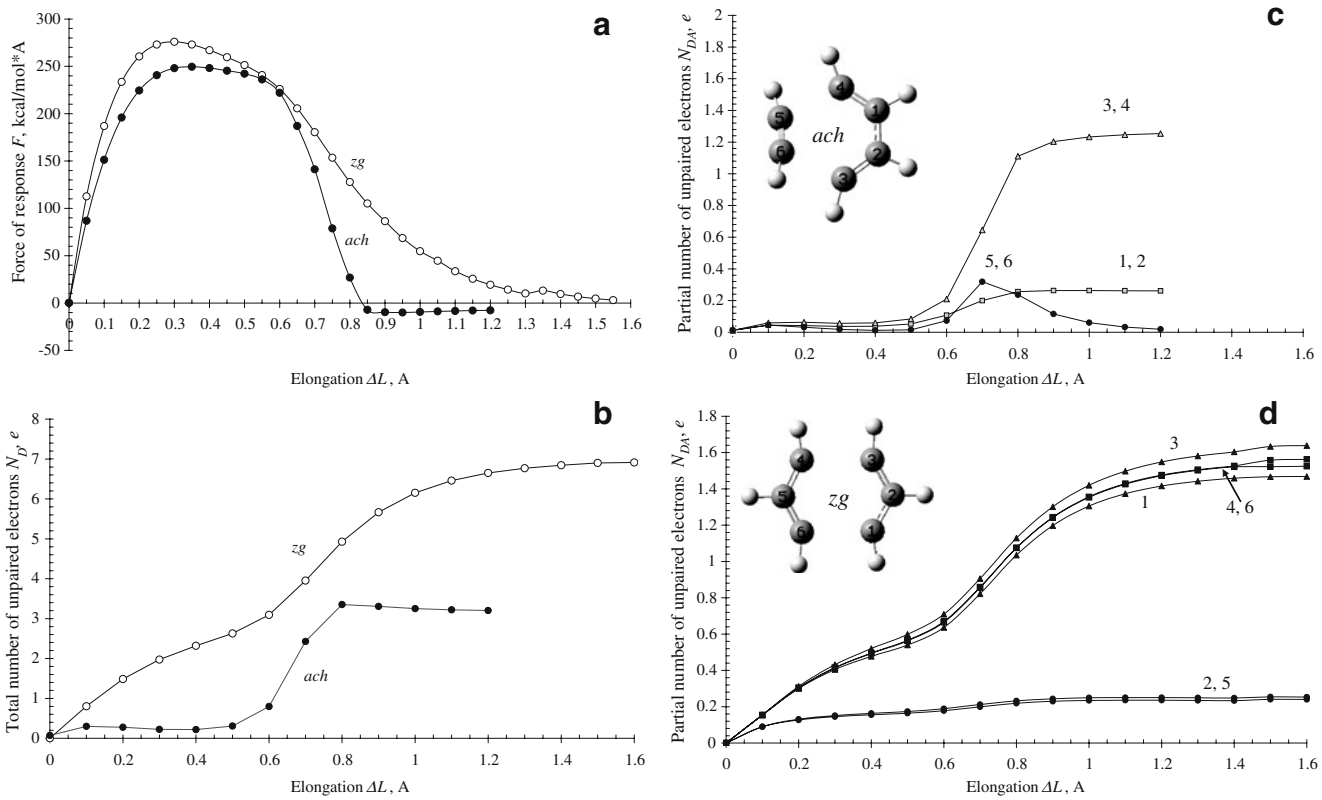

Fig. 2a–d Microscopic characteristics of the benzene molecule deformation. The numbers shown in **c** and **d** correspond to the atom number on the inserted structures and mark curves related to the relevant atoms

C_1–C_6 and C_3–C_4 molecular bonds, and two atomically identical three-atom fragments are formed under rupture. During the course of the *zg* mode, MIC elongation is immediately transformed into bond elongation. The C–C bond length of 1.395 Å in the unstrained benzene molecule is a threshold value, exceeding which violates the complete covalent coupling of the molecule odd electrons of two neighboring carbon atoms, causing the appearance of effectively unpaired electrons [24]. This explains why the increment value of 0.05 Å is significant enough for the appearance of unpaired electrons even at the first step of elongation. Bond breaking occurs when elongation achieves 0.2–0.3 Å (these very values determine the maximum position of the force-elongation dependence in Fig. 2a) but the two three-atom radicals are stabilized only when elongation exceeds 1.2 Å (see Fig. 2d).

In the case of the *ach* mode, the corresponding MICs connect atoms 1,5 and 2,6, respectively, so that ~40% of the MIC elongation is transformed into that of two C–C bonds that rest on the MIC. This explains why N_{DA} values on all carbon atoms are quite small in this case (Fig. 2c), until MIC elongation is enough to provide bond breaking. Actually, bond breaking is not a one-moment process and, as seen in Fig. 2a, it is originated at ΔL=0.3 Å and completed at ΔL=0.6 Å. Two-atom and four-atom fragments are formed when the molecule is broken. At the moment of rupture, the former is a stretched acetylene molecule. This follows from the presence of unpaired electrons on atoms 5 and 6 (see Fig. 2c) due to the relevant C–C bond length exceeding a critical value over which the covalent coupling of the odd electrons is incomplete. However, a further relaxation of the molecular structure at larger elongation shortens the bond, reducing it to below the critical value and the unpaired electrons disappear. The second fragment is a biradical whose structure is stabilized at ΔL=0.9 Å.

Therefore, the *zg* and *ach* modes of tensile deformation of benzene molecules manifest as absolutely different mechanochemical reactions. Besides the difference in the microscopic behavior, the two modes are characterized by different mechanical parameters in terms of Eqs. 2–5, whose values are given in Table 1. Taken together, the results obtained evidence a sharp mechanical anisotropy of the benzene molecule in terms of the direction of loading, as well as an extremely high stiffness of the molecule. Actually, the considered deformational modes of the benzene molecule do not reproduce exactly the similar situations for benzenoid units in CNTs and graphene; however, they do show clearly that the *zg* and *ach* edge-structure dependence of the mechanical behavior of both nanocarbons is evidently provided by the mechanical anisotropy of the units.

Tensile deformation of (5,5) nanographene

The MIC configurations of the *ach* and *zg* tensile modes of the (5,5) nanographene sheet are presented in Fig. 3. The computational procedure was fully identical to that described above for the benzene molecule, with the only difference being the step increment, δL=0.1 Å. The loading area is determined as $S = DL_{0\text{-}z(a)}$, where D is the van der Waals diameter of the carbon atom of 3.35 Å, and $L_{0\text{-}z(a)}$ is the initial length of the MICs in the case of *zg* and *ach* modes, respectively.

ach Mode of graphene tensile deformation

Figure 4 presents structure images of a selected set of deformation steps. The sheet is stretched uniformly during first 14 steps, and breaking of the first C–C bond occurs at the 15th step. Breaking is completed at the 17th step and the final structure transformation resembles that which occurs in the similar deformational mode of benzene: the sheet is divided into two fragments, one of which is a shortened (4, 5) equilibrated nanographene while the other presents a polymerized chain of acetylene molecules transferred into a carbine C = C bond chain.

Table 1 Micro-macroscopic mechanical characteristics of benzene molecule and (5,5) nanographene[a]

	Critical elongation (nm)	Critical force of response (F_{cr} N*10^{-9})	Stress σ [$(N/m^2)\times10^9$]	Stiffness coefficient (kN/m)	Young's modulus (E* TPa)
Benzene *zg* mode	0.27	12.54	153.72	46.46	3.2
Benzene *ach* mode	0.38	9.82	206.31	25.84	4.23
(5,5) graphene *zg* mode	1.47	45.08	116.18	30.66	1.14
(5,5) graphene *ach* mode	1.5	50.09	129.11	33.4	1.2
H-terminated (5,5) graphene *zg* mode	1.38	47.29	121.89	34.27	1.33
H-terminated (5,5) graphene *ach* mode	1.56	54.53	140.53	34.95	1.24

[a] Critical elongations correspond to the positions of the first zero values of the first force-of- response derivatives over the elongation. Stress and stiffness coefficients are determined at critical force of response. The Young moduli are determined as tangents of slope angles of the stress-strain curves at first steps of deformation

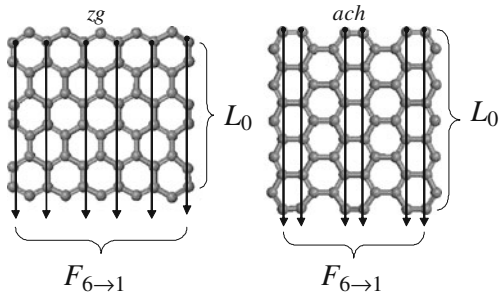

Fig. 3 Six MICs of uniaxial tension of (5,5) nanographene for the *ach* and *zg* deformational modes. L_0 Initial length of MICs, $F_{6\to1}$ six corresponding forces of response

zg Mode of graphene tensile deformation

The above illustrated mechanical anisotropy of the benzene molecule provides grounds to expect a difference in the mechanical behavior of the *ach* and *zg* tensile modes of nanographene but the results obtained greatly surpassed all our expectations. Figure 5 presents structural images of a specially selected set of successive deformation steps revealing a grandiose picture of a peculiar failure of the sheet with such a drastic difference in detail when comparing to the *ach* mode that only a simplified analogy can assist in a concise description of the picture. The failure of tricotage seems to be a proper model. Actually, as is known, the toughness of a tricotage sheet as well as the manner of its failure depends on the direction of the stress applied and the space configuration of its stitch packing. Using this analogy, each benzenoid unit represents a stitch

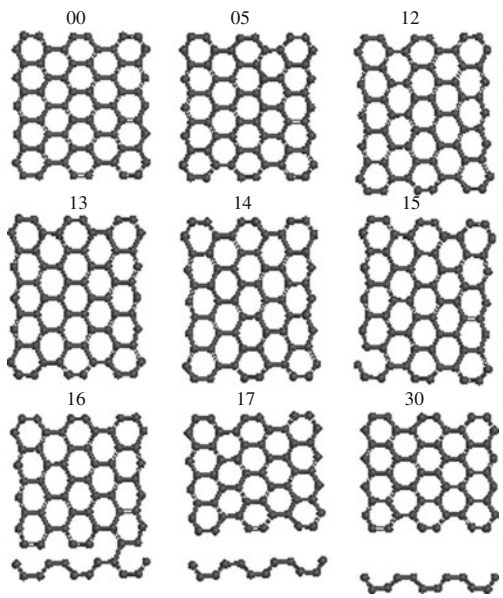

Fig. 4 Structures of (5,5) nanographene under successive steps of the *ach* regime of deformation. *Numbers* above the structures indicate step numbers

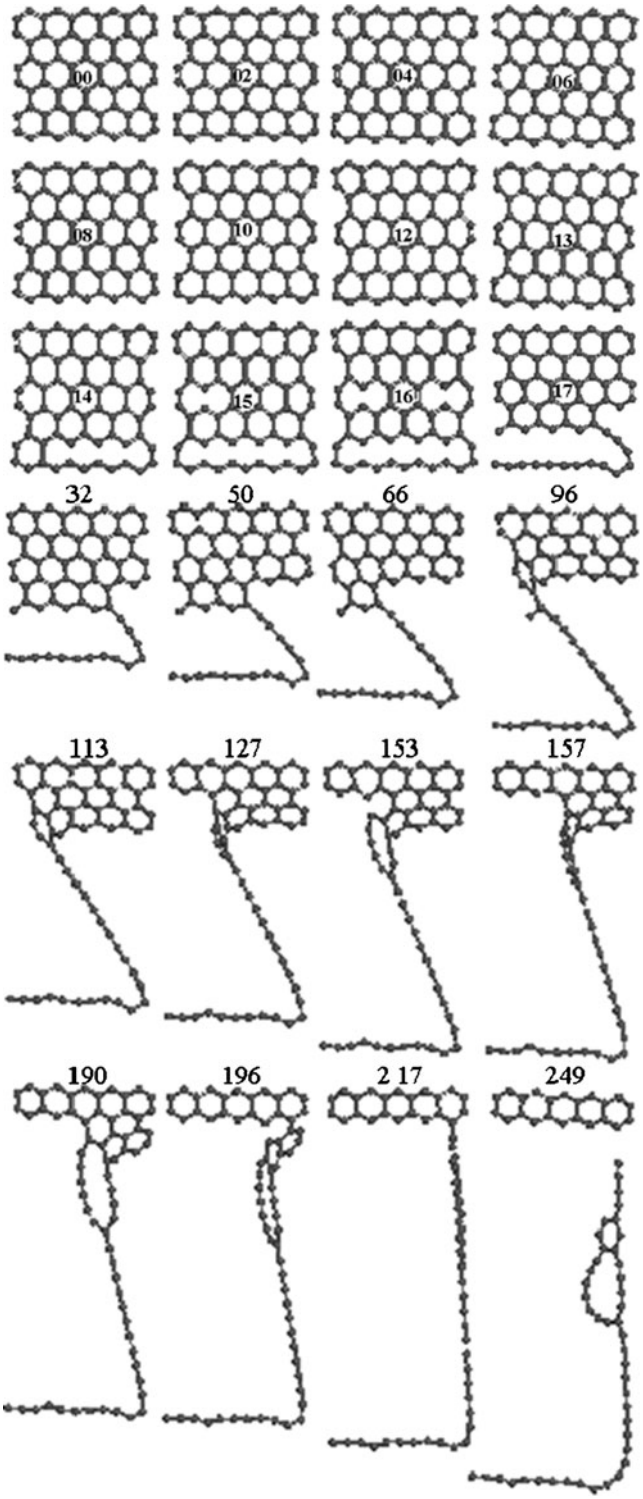

Fig. 5 Structures of the (5,5) nanographene under successive steps of the *zg* deformation regime. *Numbers* indicate the step number

and, in the case of the *ach* mode, sheet rupture both commences and is completed by the rupture of a single stitch row. In the case of the *zg* mode, the rupture of one stitch is 'tugging at thread', the other stitches being

replaced by the still elongated one-atom chain of carbon atoms. Obviously, this difference in mechanical behavior is connected with the benzenoid packing. Thus, in the *ach* deformation mode, the stitch rupture is associated with the breakage of two C–C bonds localized within one benzenoid unit, while the breaking of each C–C bond in the *zg* deformation mode touches three benzenoid units promoting the dissolution of the stitch chain in this case.

A comparative study of the *ach* and *zg* modes of the graphene tensile deformation

The difference in the structural patterns of the two deformation modes naturally leads to a difference in the quantitative characteristics of each mechanical behavior. Figure 6 shows the total forces of response and the total numbers of effectively unpaired electrons for both deformation modes versus elongation. In contrast to the benzene molecule with no unpaired electrons in the unstrained ground state, the N_D value of unstrained nanographene is quite large due to the elongation of the C–C bond of the benzenoid unit in comparison to those of the benzene molecule [15]. Figure 6b,d discloses the additional effect on the number of effectively unpaired electrons of C–C bond elongation caused by the tensile deformation. Since the calculations allow for partitioning of the N_D value over atoms, a scrupulous analysis of each bond behavior becomes possible. A detailed consideration of the topic will be presented in detail below.

As seen in Fig. 6, the microscopic behavior of nanographene at the first stage of deformation is similar to that of the benzene molecule in both cases since it is connected with scission of the first C–C bond. As seen from Table 1, the mechanical characteristics determined on the basis of the data related to the first stage of deformation are similar to those of the benzene molecule, indicating a deep connection between sheet behavior and that of the individual benzenoid unit. At the same time, all micro-macroscopic values are quite different from those of benzene, thus highlighting the influence of the unit packing on the sheet.

While the *ach* deformation is one-stage and is terminated at the 20th step, the *zg* deformation is multi-stage and proceeds up to 250 steps followed by a saw-tooth-shaped force-elongation response reflecting successive stitch dissolution, as can be seen clearly in Fig. 5, which presents structures related to the steps corresponding to the teeth maxima. In this case, only when the one-atom chain cracks at the 249th step is nanographene rupture complete. The one-atom chain fragments formed in the case of the *zg* mode of deformation have been revealed for large supercells of graphene nanoribbons in the course of DFT [14]

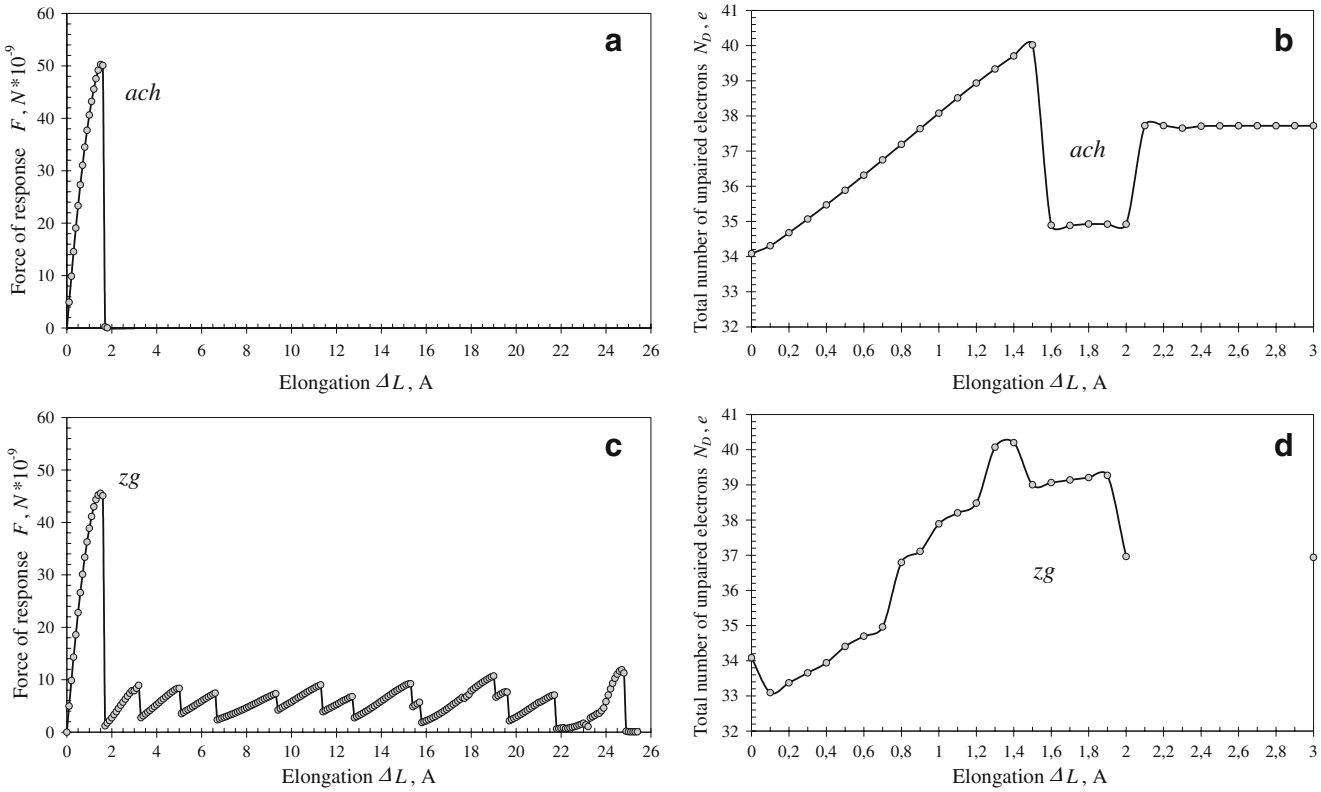

Fig. 6 Microscopic characteristics of (5,5) nanographene deformation

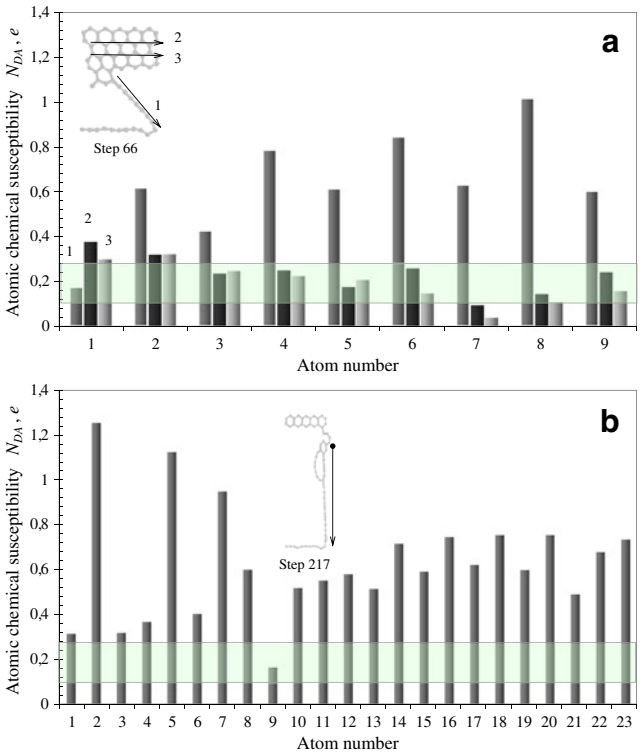

Fig. 7 Atomic chemical reactivity within selected atom sets (marked by *arrows*)

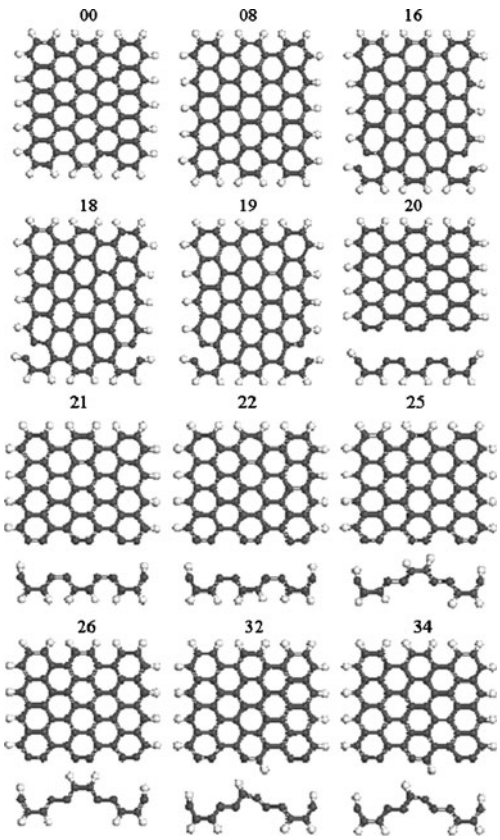

Fig. 8 Structures of H-terminated (5,5) nanographene under successive steps of the *ach* regime of deformation. *Numbers* indicate step number

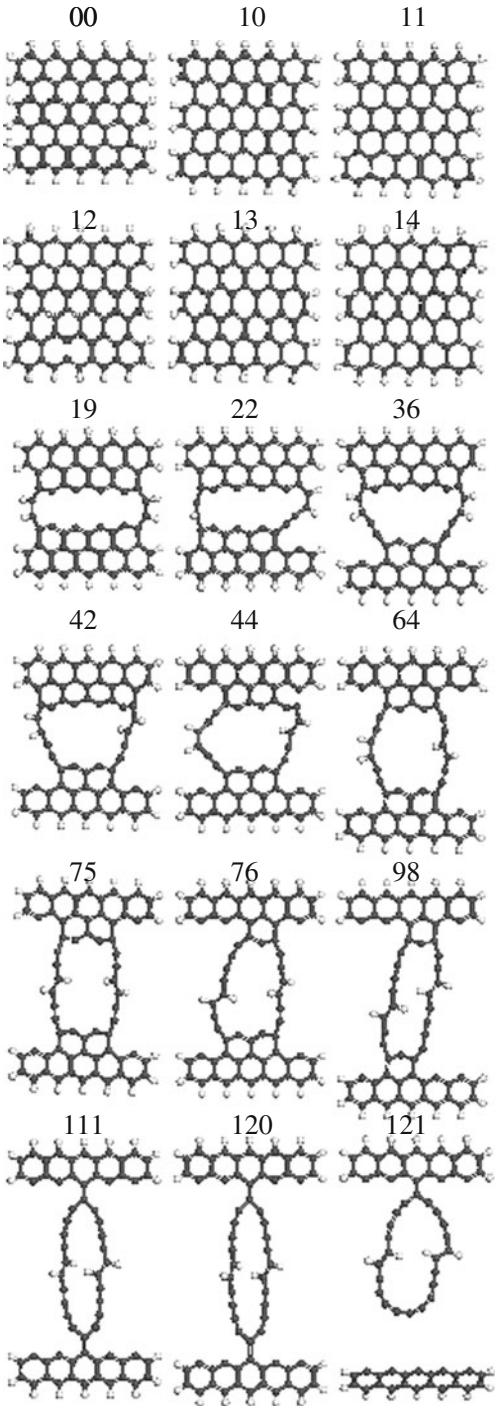

Fig. 9 Structures of H-terminated (5,5) nanographene under successive steps of the *zg* regime of deformation. *Numbers* indicate step number

and molecular dynamics [11] calculations. This tendency towards formation of one-atom chains under stress has also been recently recorded experimentally [27, 28]. As seen in the figures presented in the literature, and in particularly in a movie accompanying one report [29], experimentally observed formation of the one-atom carbon chain occurs in

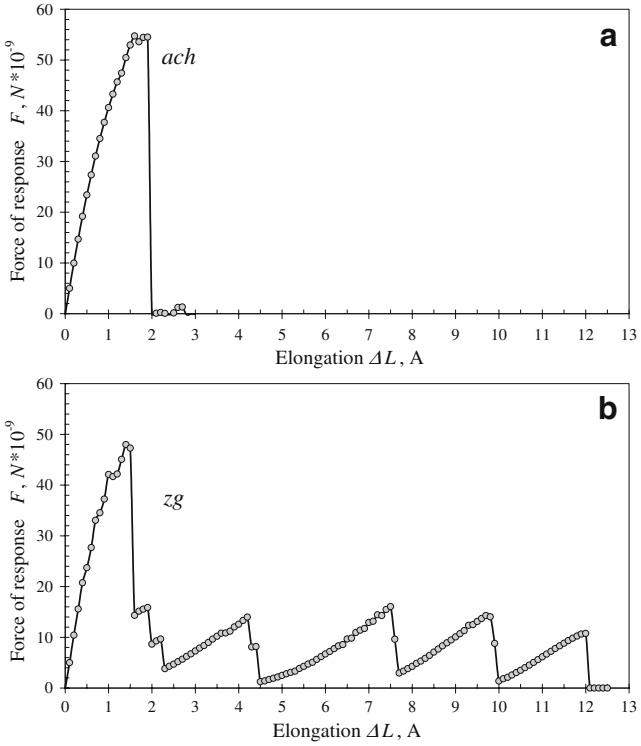

Fig. 10 Total force-elongation response of H-terminated (5,5) nanographene under *ach* (**a**) and *zg* (**b**) modes of deformation

the manner predicted by the *zg* mode of deformation. It seems reasonable to suggest that just the stress originating during electron beam bombardment of the graphene body is sufficient to cause this peculiar structural transformation, creating these one-atom chains of carbons.

The N_D dependencies shown in Fig. 6b,d clearly evidence the difference in the mechanochemical reactions related to the *ach* and *zg* deformation modes even at the first stage. While the reaction is terminated after achieving the 21st step in the former case, the *zg* reaction proceeds further with the N_D dependence resembling a saw-tooth pattern characteristic of the response force in Fig. 6c. It is important to note that the discussed N_D dependencies reflect a quantitative change in the chemical reactivity of the nanographene sheet under tensile deformation. This is particularly attributed to one-atom chains. Figure 7a discloses the distribution of the atomic chemical susceptibility, N_{DA}, over three sets of atoms related to the structures at the 66th step of deformation. The first set joins atoms of the chain (arrow 1). The other two atom rows are located inside the fragment, which still retains the graphene configuration (arrows 2 and 3). The shaded block covers the interval of the N_{DA} values characteristic for pristine nanographene [15]. As seen in the figure, the chemical reactivity of atoms inside rows 2 and 3 differ only slightly from the pristine data, while atoms of the one-atom chain are highly radicalized. This radicalization is conserved and even strengthened at final steps of deformation as shown in Fig. 7b.

Tensile deformation of hydrogen-terminated (5,5) nanographene

The termination of (5,5) nanographene sheet edges by hydrogen atoms, preserving a qualitative picture of nanographene mechanical behavior in general, changes drastically in details. Figures 8 and 9 present the final structures related to the *ach* and *zg* deformation modes that are accomplished at the 20th and 122th steps, respectively. The corresponding force-elongation response is shown in Fig. 10. In the case of the *ach* mode, like that of non-terminated graphene, deformation occurs in one stage, with the only difference concerning the structure of the final fragments, which is influenced by the presence of hydrogen atoms. In contrast, in the *zg* mode, although multi-stage as previously, proceeds nevertheless quite differently compared to the non-terminated graphene. The first C–C bond broken is located right in the center of the sheet so that further bond scission leads to the formation of a closed one-atom chain of carbon atoms, whose splitting as a whole (see Fig. 9, step 121) from the nanographene edge manifests the termination of sheet failure. Although this action occurs at the 121st step, i.e., at

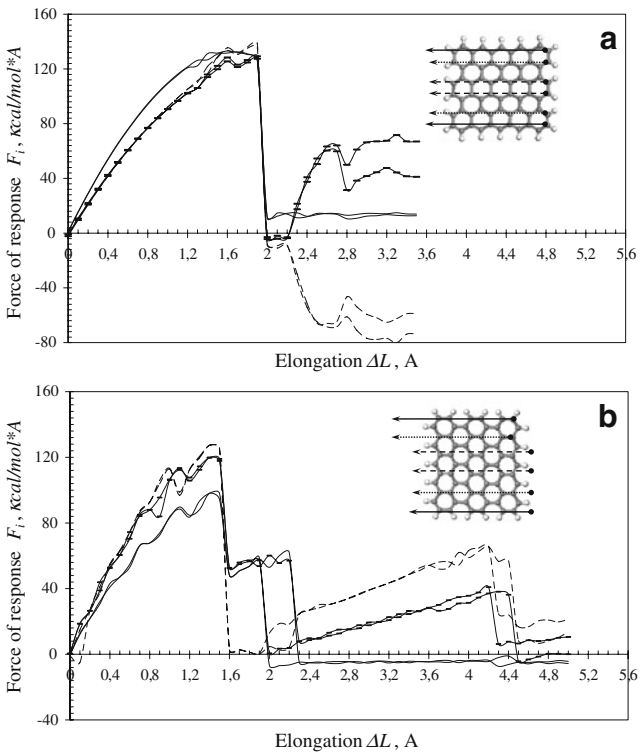

Fig. 11 Force-elongation response of H-terminated (5,5) nanographene in relation to each of the six MICs under *ach* (**a**) and *zg* (**b**) modes of deformation. The plotted traces correspond to the MICs illustrated

far longer elongation than that of the *ach* mode, the latter is half that of the non-terminated graphene.

With both deformation modes, the N_{DA}-elongation response for H-terminated graphene behaves quite similarly to that of non-terminated graphene, reflecting C–C bond elongation by increasing the N_{DA} values as well as pointing to a high radicalization of the atoms that form the one-atom chain. This similarity also concerns the force-elongation response related to each of the six MICs shown in Fig. 3. Figure 11 presents the related curves for H-terminated graphene. The six components shown in the figure constitute the total forces of response presented in Fig. 10, and illustrate how complicated the graphene failure process is in reality.

Table 1 collects the main parameters related to the first stage of deformation; within this stage, there is an obvious similarity in the behavior of both non-terminated and H-terminated sheets under both deformation modes. The Young moduli data are within the range determined by other calculations [11] and correlate with the 1 TPa suggested on the basis of experimental observations [29]. However, it should be noted that the region of elongation that supports the linear elastic law is rather short in all cases, so that, from the very beginning, graphene deformation is nonlinear and apparently non-elastic. This fact poses the first question about the possibility of describing graphene deformation on the basis of the theory of elasticity by using such parameters as Young moduli, Poisson coefficients, and so forth. The second question follows from the fact that the one-stage deformation that is usually implied within the theory of elasticity viewpoint occurs only in the case of the *ach* mode. In contrast, *zg* deformation is multi-stage, which places it completely outside the theory of elasticity, and deprives the parameters of any sense. At the same time, the data related to the first stage, i.e., the largest, scale the loading that needs to be applied to graphene for failure to occur.

Conclusions

The QCh mechanochemical-reaction approach has proved highly effective in revealing the atomically matched peculiarities that accompany the deformation-failure-rupture process occurring in nanographenes. As demonstrated, a high degree of stiffness of the graphene body correlates with that of the benzenoid unit. The anisotropy of the mechanical behavior of the unit, in combination with different packing of the units either normally or parallel to the body C–C bond chains, forms the basis of the structure-sensitive mechanism of the mechanical behavior of the object, which depends entirely on the deformation mode. The mechanical behavior of graphene under *zg* and *ach* deformation modes is similar to that of a tricotage when either the sheet rupture is both commenced and completed by the rupture of a single stitch row (*ach* mode), or the rupture of one stitch is 'tugging at thread' so that the other stitches are replaced by an elongated one-atom chain of carbon atoms (*zg* mode). For the first time, this approach allows tracing of deformation-stimulated change in the chemical reactivity of both nanographene sheet as a whole and its individual atoms in terms of total and partial numbers of effectively unpaired electrons. The peculiarities of graphene deformation described here reveal the necessity of a serious reexamination of the modern versions of the theory of elasticity adapted for each case.

References

1. Kudin K, Scuseria GE, Yakobson BI (2001) C_2F, BN, and C nanoshell elasticity from ab initio computations. Phys Rev B 64:235406–235410
2. Liu F, Ming P, Li J (2007) Ab initio calculation of ideal strength and phonon instability of graphene under tension. Phys Rev B 76:064120–064127
3. Hemmasizadeh A, Mahzoon M, Hadi E, Khadan R (2008) A method for developing the equivalent continuum model of a single layer graphene sheet. Thin Solid Films 516:7636–7640
4. Wei X, Fragneaud B, Marianetti CA, Kysar JW (2009) Nonlinear elastic behavior of graphene: ab initio calculations to continuum description. Phys Rev B 80:205407–205408
5. Shokrieh MM, Rafiee R (2010) Prediction of Young's modulus of graphene sheets and carbon nanotubes using nanoscale continuum mechanics approach. Mater Des 31:790–795
6. Li C, Chou TW (2003) A structural mechanics approach for the analysis of carbon nanotubes. Int J Solids Struct 40:2487–2499
7. Sakhaee-Pour A (2009) Elastic properties of single-layered graphene sheet. Solid State Commun 149:91–95
8. Hashemnia K, Farid M, Vatankhah R (2009) Vibrational analysis of carbon nanotubes and graphene sheets using molecular structural mechanics approach. Comput Mater Sci 47:79–85
9. Tsai JL, Tu JF (2010) Characterizing mechanical properties of graphite using molecular dynamics simulation. Mater Des 31:194–199
10. Guo Y, Guo W (2003) Mechanical and electrostatic properties of carbon nanotubes under tensile loading and electric field. J Phys D Appl Phys 36:805–811
11. Bu H, Chen Y, Zou M, Yi Y, Ni Z (2009) Atomistic simulations of mechanical properties of graphene nanoribbons. Phys Lett A 373:3359–3362
12. Van Lier G, van Alsenoy C, van Doren V, Geerlings P (2000) Ab initio study of the elastic properties of single-walled carbon nanotubes and graphene. Chem Phys Lett 326:181–185
13. Gao Y, Hao P (2009) Mechanical properties of monolayer graphene under tensile and compressive loading. Physica E 41:1561–1566
14. Topsakal M, Ciraci S (2010) Elastic and plastic deformation of graphene, silicene, and boron nitride honeycomb nanoribbons under uniaxial tension: a first-principles density-functional theory study. Phys Rev B 81:024107
15. Sheka EF, Chernozatonskii LA (2010) Broken spin symmetry approach to chemical susceptibility and magnetism of graphenium species. J Exp Theor Phys 110:121–132

16. Tobolski A, Eyring H (1943) Mechanical properties of polymeric materials. J Chem Phys 11:125–134
17. Dewar MJS (1971) MO theory as a practical tool for studying chemical reactivity. Fortschr Chem Forsch 23:1–63
18. Nikitina EA, Khavryutchenko VD, Sheka EF, Barthel H, Weis J (1999) Deformation of poly(dimethylsiloxane) oligomers under uniaxial tension. Quantum-chemical view. J Phys Chem A 103:11355–11365
19. Khavryutchenko V, Nikitina E, Malkin A, Sheka E (1995) Mechanics of nanoobjects. Computational mechanochemistry. Phys Low-Dimens Struct 6:65–84
20. Khavryutchenko VD, Khavryutchenko AV Jr (1993) DYQUAMECH dynamical-quantum modelling in mechanochemistry. Software for personal computers. Institute of Surface Chemistry, National Acadamy of Sciences of the Ukraine, Kiev
21. Zayets VA (1990) CLUSTER-Z1: Quantum-chemical software for calculations in the s, p-basis. Software for personal computers. Institute of Surface Chemistry, National Acadamy of Sciences of the Ukraine, Kiev
22. Sheka EF, Chernozatonskii LA (2010) Broken symmetry approach and chemical susceptibility of carbon nanotubes. Int J Quantum Chem 110:1466–1480
23. Pulay P, Fogarasi G, Pang F, Boggs JE (1979) Systematic ab initio gradient calculation of molecular geometries, force constants and dipole moment derivatives. J Am Chem Soc 101:2550–2560
24. Sheka EF (2007) Chemical susceptibility of fullerenes in view of Hartree-Fock approach. Int J Quantum Chem 107:2803–2816
25. Popova NA, Sibgatullina LKh, Sheka EF, Nikitina EA (2009) Quantum-chemical study of deformation mechanism of carbon nanotubes. Abstracts of the Second International Nanoforum, Rosnanotech, pp 169–171
26. Sheka EF, Popova VA, Popova NA, Nurullina LKH, Nikitina EA (2009) Mechanism of structure-sensitive fracture of nanographene. Abstracts of the Second International Nanoforum. Rosnanotech, pp 166–168
27. Chuvilin A, Meyer JC, Algara-Siller G, Kaiser U (2009) From graphene constrictions to single carbon chains. New J Phys 11:083019
28. Jin C, Lan H, Pen L, Suenaga K, Iijima S (2009) Deriving carbon atomic chains from graphene. Phys Rev Lett 102:205501–205504
29. Lee C, Wei X, Kysar WJ, Hone J (2008) Measurement of the elastic properties and intrinsic strength of monolayer graphene. Science 321:385–388